JOURNAL OF MATERIALS SCIENCE 32 (1997) 4153–4158

A study on the low-cycle fatigue properties of SiC_p/6061 Al composites

PERNG-CHENG CHEN, SU-JIEN LIN
Department of Materials Science and Engineering, National Tsing Hua University, Hsinchu, Taiwan
MIN-TEN JAHN
Mechanical Engineering Department, California State University, Long Beach, CA, 90840, USA

Metal matrix composites (MMCs) were produced using a powder metallurgy method. Fatigue and tensile specimens were extruded and rolled before being machined. The matrix of the composite was a 6061 Al alloy and the reinforcement was 180 mesh SiC particle (SiC_p). Different weight fractions (10, 20 and 30 wt %) of 180 mesh SiC_p were introduced to determine the influence of the SiC_p content on the tensile and low-cycle properties. Reasonable Coffin–Manson plots have been obtained in low-cycle fatigue. More accountable data of fatigue ductility exponents and fatigue ductility coefficients have been obtained for the composites and monolithic Al alloy. Increasing the content of SiC_p has been shown to encourage the development of particle cracks and resulted in the degradation of fatigue properties.

1. Introduction

In recent years metal matrix composites (MMCs) have received increasing attention due to their excellent combination of physical and mechanical properties such as a low density, high specific strength, high elastic modulus and a desirable coefficient of thermal expansion. When composites are exposed to high temperatures MMCs are superior to polymer matrix composites. MMCs have been increasingly found application in the aerospace and defence sectors. The airframe of the USA National Aerospace Plane Vehicle (X-30) will be produced from a silicon carbide-reinforced titanium alloy since it can sustain temperatures up to 800 °C [1]. Various forms of reinforcements are used in composites including continuous fibres, discontinuous fibres, whiskers, nodules and particulates. While the aligned continuous fibre-reinforced composites provide a higher specific strength and elastic modulus, the particulate-reinforced composites possess some advantages, for example they are more isotropic because the distribution and shape of the reinforcements are generally random. Besides, with some modifications, the conventional manufacturing process for metals and alloys such as casting, forging, extrusion, rolling and powder metallurgy can be applied to produce the particulate-reinforced composites [2].

In the development and design of new structural materials fatigue behaviour is an important factor that must be considered. Fatigue failure takes place frequently with more than 90 % of premature failures of dynamic components in structures such as motor vehicles, aircraft, compressors and engines being due to fatigue. The prevention and prediction of fatigue are especially important if the components are made of brittle materials since the fatigue failure can be catastrophic and can occur without any warning. Since in general MMCs show a lower tensile ductility than their counterpart matrix materials [3, 4], comprehensive study of the fatigue behaviour of MMCs is essential for their design and application. It has been reported that the presence of reinforcements in MMCs degrades the low-cycle fatigue characteristics when the MMCs are subject to strain-controlled cyclic loading [5, 6]. Many factors are involved in the degradation, they include the brittle nature of reinforcements, plastic-flow constraint of the matrix due to the presence of the reinforcements, stress concentration, dislocation density near the interface and the hydrostatic stresses within the constrained matrix [5, 7, 8].

A considerable number of investigations into the fatigue behaviour of MMCs have been performed [5–12] in recent years. The cyclic strain hardening of whisker-reinforced composites and particulate-reinforced composites have been analysed using numerical methods and compared with experimental results by Llorca *et al.* [8]. They have reported that increasing the volume fraction of SiC particulates in an Al alloy promotes higher tensile stresses in the reinforcements and, accordingly, a higher degree of particle fracture takes place [8]. Vyletel *et al.* [9] have shown that the fatigue life of the composite material (TiC particulates in an Al alloy) was independent of the precipitate type (shearable or nonshearable) in either stress-controlled or plastic strain controlled testing. The crack initiation and growth (or linkage of small cracks) during

0022–2461

low-cycle fatigue of discontinuously reinforced MMCs have been examined by several authors [5, 6, 12]. Most results indicated that particle cracks and/or particle decoherences were the main sources of fatigue crack initiation. Despite the great number of investigations into the fatigue behaviour of MMCs, we are still far from a complete understanding of this behaviour. In this study we examine the effect of varying the weight fraction of SiC particulates in a 6061 Al alloy matrix on the fatigue properties such as cyclic hardening/softening, crack initiation and growth, fracture surface morphology and fatigue life. The SiC particulates used here were much larger (median size 85 μm) than used previously (median size 3–10 μm) [5–9] for clearer investigation. It is believed that more insights and a more systematic study into fatigue crack initiation, growth, cyclic work hardening/softening and particulate volume fraction effect on fatigue life are presented in this study.

2. Experimental procedure

In this investigation, the matrix used was commercial Al–Mg–Si 6061 Al alloy, and the reinforcement was SiC_p. The chemical composition and powder characteristics of the Al alloy and SiC_p are shown in Tables I and II, respectively.

First, different weight fractions of 6061 Al alloy powder and SiC_p powder were mixed homogeneously, then the mixed powder was poured into a plastic mould which was inserted into a vacuum tube and the air was evacuated until a vacuum of 1.333×10 Pa was reached. Finally, the mould was sealed up with a rubber cover, and cold isostatic pressed (CIP) at 50, 100, and 200 MPa, respectively, to produce an ingot of the composite. Increasing the CIP pressure produced a higher densification of the ingot. However, the fraction of closed pores inside the ingot, which is detrimental to degassing and dewaxing, also increased. When the ingot was compressed under a 200 MPa CIP pressure, there were very few open pores. The optimum pressure was determined to be 100 MPa.

The ingots were placed in an air furnace at 400 °C for 4 h to remove the air and wax. They were then put into a controlled atmosphere furnace under an argon flow for liquid phase sintering at 620 °C for 6 h followed by air cooling to room temperature. The sintered ingot was extruded at 500 °C to a ratio of 9 : 1. The extruded products were rolled from 4 to 3 mm at room temperature in accordance with the thickness of the specimens. Fig. 1(a–c) reveals that the distribution of SiC_p in the composite is rather uniform after extrusion.

TABLE II Composition and particle size of the SiC_p

Composition (wt %)	SiC 99.2	FeO 0.008	F.C 0.11
Average particle size (μm)	85		
Density ($g\,cm^{-3}$)	3.2		

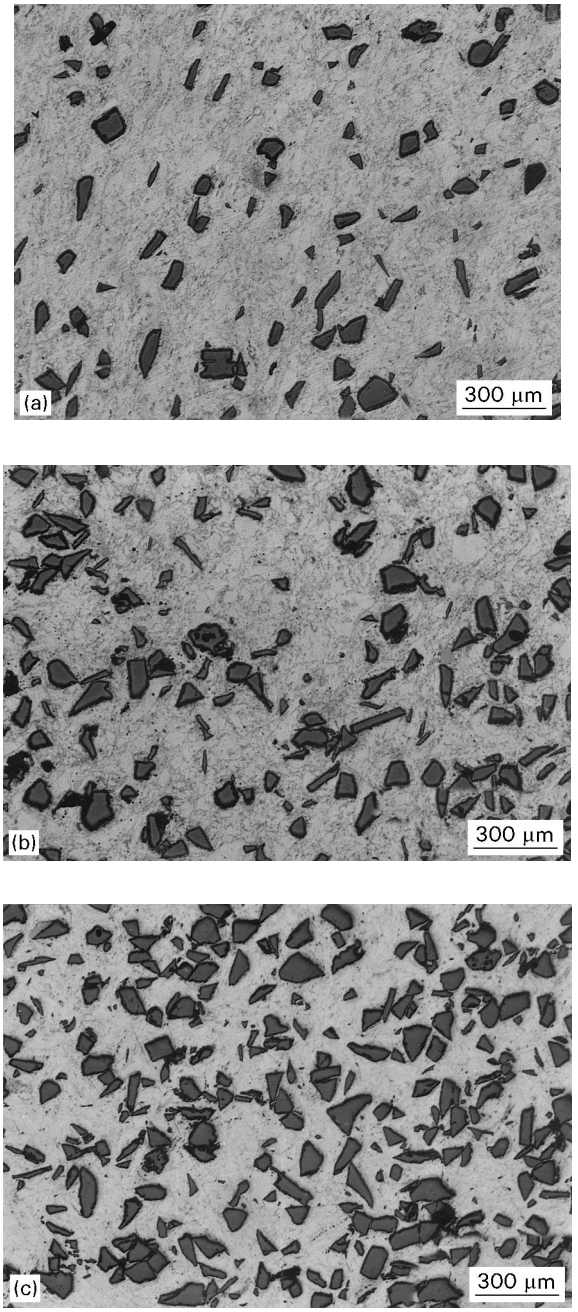

Figure 1 Optical micrographs of composites after extrusion: (a) 10 wt %, (b) 20 wt % and (c) 30 wt % SiC_p.

TABLE I Composition and particle sizes of the 6061 Al alloy powder

Composition (wt %)	Al	Fe	Si	Cu	Mg	Acrawax
	98.00–98.03	0.09	0.61–0.62	0.29	0.95–0.97	1.50–1.51
Average particle size (μm)	93					
Apparent density ($g\,cm^{-3}$)	1.21–1.22					
Theoretical density ($g\,cm^{-3}$)	2.7					

TABLE III Tensile property data

	Yield stress (MPa)	UTS (MPa)	Elastic modulus (GPa)	Elongation (%)
6061 Al	269	318	68.8	8.6
6061 Al + 10 wt % SiC_p	296	327	83.5	4.5
6061 Al + 20 wt % SiC_p	338	359	98.2	1.3
6061 Al + 30 wt % SiC_p	331	349	113.7	< 1

Test specimens of the composites and the unreinforced 6061 Al alloy with a 6 mm width, 9 mm gauge length and 3 mm thickness were solution-treated at 530 °C for 1 h and then water quenched. Subsequently, the composites and the 6061 Al alloy were aged at 175 °C for 8 h (T6). After this T6 treatment, the specimens were polished with SiC papers of various grades ranging from 240 to 1200 grit.

Then the specimens were stored in a freezer while not being used in order to prevent possible natural ageing. The yield strength, tensile strength, Young's modulus and elongation were measured by a closed-loop servo-hydraulic MTS machine. The stress axis of fatigue and tensile tests was parallel to the extrusion direction. The results of the tensile tests are listed in Table III.

The low-cycle fatigue (LCF) test with a fatigue life of less than 10^4 cycles was carried out using an MTS machine. The fully reversed uniaxial fatigue tests were performed under strain control at room temperature with an imposed triangular waveform strain rate of $10^{-3}\,s^{-1}$. Multiple-step, strain-controlled fatigue load was used to determine the cyclic hardening/softening behaviour, and stable stress–strain hysteresis loops. This procedure was continued until complete failure of the specimen occurred.

The fracture surfaces of the specimens after fatigue testing were examined using a scanning electron microscope (SEM). Sections of the specimens after fatigue testing at different strain amplitudes were selected to study the characteristics of the fatigue crack initiation and growth.

3. Results and discussion

3.1. Densification

The densification of composites containing mesh 180 (85 μm) SiC_p reinforcement is listed in Table IV. Increasing the SiC_p content tended to reduce the densification of the green compact of the composite. The reason for this could be that reinforcement particles restrict the flow of the 6061 Al alloy powder, and the porosity of the SiC_p clustering is harder to eliminate during sintering if the SiC_p fraction is higher. As shown in Fig. 1(a–c), the particles were homogeneously distributed with good bonding in the interface and practically without any voids over the whole section.

TABLE IV Densification of 6061 Al alloy and the composites

Material	Density ($g\,cm^{-3}$)	Theoretical density ($g\,cm^{-3}$)	Densification (%)
6061 Al	2.349	2.700	87.0
6061 Al + 10 wt % SiC_p	2.382	2.743	86.8
6061 Al + 20 wt % SiC_p	2.377	2.787	85.3
6061 Al + 30 wt % SiC_p	2.380	2.833	84.0

3.2. Tensile properties

The tensile test is the basis of the fatigue test. The relationship between stress and strain can be used to predict the level of the relative cyclic stress–strain. As shown in Table III, SiC_p reinforcement promotes stiffness and strength at the expense of elongation. Note that the 30 wt % SiC_p composite was too brittle to accurately measure the yield and tensile strengths. The observed low ductility and high strength values are due to the combined effects of brittle reinforcement particles, constraint of plastic deformation in the matrix by SiC_p, and more dislocation density at the SiC_p/Al interface due to thermal mismatch between the matrix and SiC_p when the composite was water quenched.

3.3. Low-cycle fatigue properties

The weight fraction of SiC_p influenced the fatigue life. For the strain-controlled fatigue test, the plastic strain can be obtained from the saturated stress–strain loop. The fatigue strain versus life curve was obtained from the plastic strain amplitude and reversals to failure ($2N_f$) using bi-logarithmic co-ordinates. The straight line fit for the strain amplitude–fatigue life curve can be obtained by linear regression analysis. The regression curve was calculated and compared with the Coffin–Manson equation [13,14]:

$$1/2\,\Delta\varepsilon_p = \varepsilon_f'(2N_f)^c \quad (1)$$

where $1/2\Delta\varepsilon_p$ is the plastic amplitude obtained from the saturated stress–strain loop, ε_f' is the fatigue ductility coefficient, c is the fatigue ductility exponent, and $(2N_f)$ is the number of reversals to fatigue failure.

Fig. 2 represents the variation of fatigue-life cycles with plastic strain amplitude for composites with various SiC_p contents. The fatigue ductility exponent c is the slope of the regression curve, and the fatigue ductility coefficient ε_f' is the intercept of the curve with vertical axis at $2N_f = 1$. It is obvious that the larger the absolute value of c, the steeper the curve, resulting in poorer fatigue properties. The value of the coefficient ε_f' also indicates the material's resistance to fatigue failure. A higher ε_f' value at the same value of c represents better fatigue resistance. Therefore, a higher value of ε_f' and a lower absolute value of c are required for stronger resistance to fatigue failure.

As shown in Fig. 2, the straight line for the 6061 Al alloy is above the other three straight lines for the composites, therefore, the 6061 Al alloy has the best fatigue resistance. The absolute value of c for the 6061 Al alloy is the smallest and ε_f' is only slightly smaller

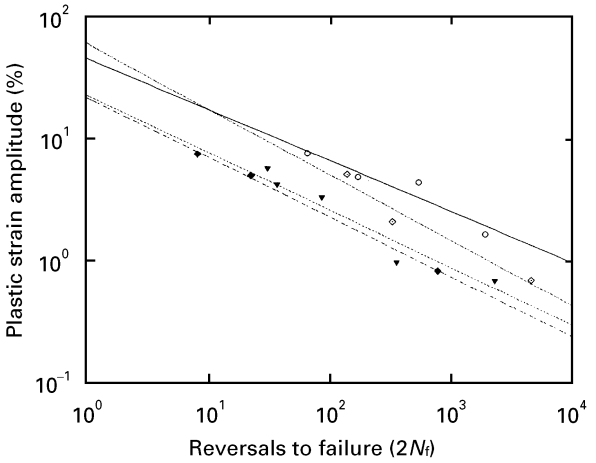

Figure 2 Variation of fatigue-life cycle with plastic strain amplitude for composites with various SiC_p contents. Key: (○) 6061 alloy, $c = -0.416$, $\varepsilon_f' = 4.5\%$, (◇) 180 mesh 10 wt % SiC_p/6061 Al, $c = -0.535$, $\varepsilon_f' = 5.91\%$, (▼) 180 mesh 20 wt % SiC_p/6061 Al, $c = -0.470$, $\varepsilon_f' = 2.26\%$ and (◆) 180 mesh 30 wt % SiC_p/6061 Al, $c = -0.489$, $\varepsilon_f' = 2.16\%$.

than the 10 wt % SiC_p/6061 Al composite, yet it is much larger than the 20 and 30 wt % SiC_p/6061 Al composites. Besides, the 10 wt % SiC_p/6061 Al composite is superior to the 20 and 30 wt % SiC_p/6061 Al composites for the low-cycle fatigue regime which is principally due to its much higher ε_f' value. Comparing the fatigue properties of the 20 and 30 wt % SiC_p/6061 Al composites, the 20 wt % SiC_p/6061 Al composite has the largest ε_f' and a lower absolute value of c. Therefore, the 20 wt % SiC_p/6061 Al composite has a better fatigue resistance than the 30 wt % SiC_p/6061 Al composites. The ε_f' values did not closely accord with the monolithic ductility represented by plastic strain at failure. However, the values exhibited a plausible tendency.

The fatigue properties of the MMCs obtained in previous studies are listed concurrently with the data obtained in this study in Table V. In theory, a higher value of ε_f' represents better ductility (represented by elongation El) of the material. The results of Srivatsan [5] show contradictory behaviour between ε_f' and El, in that the higher the El the lower the ε_f'. However, the ε_f' and El obtained in this study indicate general agreement between each other, that is a higher El generally leads to a higher ε_f'. However, the results of Srivatsan [5] and this study both reveal that a greater content of SiC_p in the composite results in a worse fatigue resistance measured using a strain-controlled fatigue test. In comparison with the results of Levin and Karlsson [6], the fatigue resistance for SiC_p/6061 Al MMCs is better in this study because of the lower absolute values of c and higher ε_f' values. Levin and Karlsson [6] have suggested that the presence of 20 vol % of alumina short fibres in the 6061 Al alloy degraded the fatigue resistance of the MMCs, but the fatigue resistance of 15 vol % SiC_p/6061 Al is superior to monolithic 6061 Al alloy. This is contradictory to the generally accepted viewpoint that the presence of reinforcement in MMCs degrades the low-cycle fatigue property when the MMCs are subject to strain-controlled cyclic loading [5, 7, 8]. The results obtained in this study closely agree with the generally held viewpoint.

The particle size of the reinforcement used in this study is larger than that used by Srivatsan [5] and Levin and Karlsson [6]; accordingly, the fatigue property obtained should be worse than that of Srivatsan [5] and Levin and Karlsson [6] at the same volume fraction of SiC_p. The reasons for this behaviour are that the larger reinforcement particle contains more defects, and the stress concentration is larger while a crack is propagating to a particle. So, it seems easier for a large particle to crack and for the crack to propagate. However, it can be seen that the experimental results obtained in this study are better than those of Levin and Karlsson [6]. One possible explanation is that the finer particles used by Levin and Karlsson [6] resulted in clustering, which can easily initiate fatigue cracking because of the poor bonding between the clustering particles and the matrix. The matrix used in this study was different from the one used by Srivatsan [5], therefore the fatigue resistance values cannot be compared but we note that the relationship between ε_f' and elongation is not as consistent as that obtained in this study. The reason for this behaviour could be that the reinforcement particles are distributed more homogeneously in this

TABLE V Fatigue properties

Matrix	SiC_p fraction	Medium particle size (μm)	Fatigue ductility exponent c	Fatigue ductility coefficient ε_f' (%)	Elongation (%)	Reference
6061	10 wt % (8.57 vol %)	85	− 0.535	5.91	4.5	This study
6061	20 wt % (17.4 vol %)	85	− 0.470	2.26	1.3	This study
6061	30 wt % (26.6 vol %)	85	− 0.489	2.16	< 1.0	This study
6061	0	NA	− 0.416	4.50	8.6	This study
2124	20 vol %	~8	− 0.16	0.76	6.7	[5]
2124	25 vol %	~8	− 0.25	1.33	6.0	[5]
2124	30 vol %	~8	− 0.55	6.78	4.2	[5]
6061	15 vol %	~10	− 0.58	0.041	NA	[6]
6061	0	NA	− 0.93	0.21	NA	[6]

study. Therefore, the homogeneity as well as good bonding in this study lead to results which are more self consistent.

3.4. Cyclic stress response

The low-cycle fatigue experiments performed in this study revealed that a hardening effect was observed for both the 6061 Al alloy and its composites during the first several or several tens of cyclic strains. For 6061 Al, which is a precipitation-hardened alloy, the interaction between the dislocations and the matrix precipitates would result in a softening effect [15]. However, the increase in the response stress amplitude during the fatigue cycling means that the hardening contribution from the interaction amongst dislocations (work hardening) dominates over softening [16]. The hardening phenomenon for the composites in this study occurred only during the initial cycles, which is different from the cyclic-hardening effect observed by Srivatsan [5] and Srivatsan *et al.* [7] which continued during all of the fatigue cycling until sudden softening which led to final fracture. After several or several tens of cycles in this study, the dislocation integrated effect (dynamic recovery) balances the hardening phenomenon, and so the specimens exhibit a steady-state behaviour for the stress response. Finally, the rapid fracture occurred when microscopic cracks combined to form macroscopic cracks.

3.5. Fracture surface

An SEM micrograph of a fatigue-fractured surface for the 6061 Al alloy is shown in Fig. 3. It is typically observed that a ductile fracture with plenty of dimples exists for the unreinforced alloy. In addition, some secondary cracks were also observed, which is not uncommon for materials made by a powder metallurgy method.

The morphology of the fatigue-fractured surface for the composite is obviously different from the monolithic Al alloy. The fracture surfaces of the composites are shown in Fig. 4 (a–c). For a 10 wt % SiC_p/6061 Al composite there are clearly tiny inclusions embedded in dimples in the matrix, which indicates that the decohesion or split of SiC_p causes the crack initiation. For the 20 and 30 wt % SiC_p/6061 Al composites the fracture surface contains particle splits, but little decohesion and few dimples. The fracture of the large particles (180 mesh SiC_p) was almost all of the cleavage failure type. Therefore, increasing the content of SiC_p leads to shortcut crack propagation and results in worse fatigue resistance.

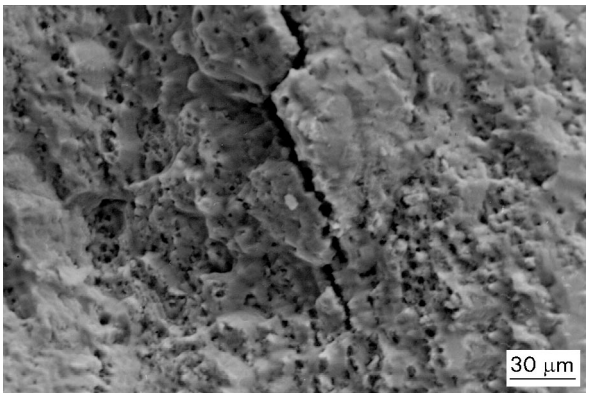

Figure 3 SEM micrograph of an 6061 Al alloy fatigue fracture surface.

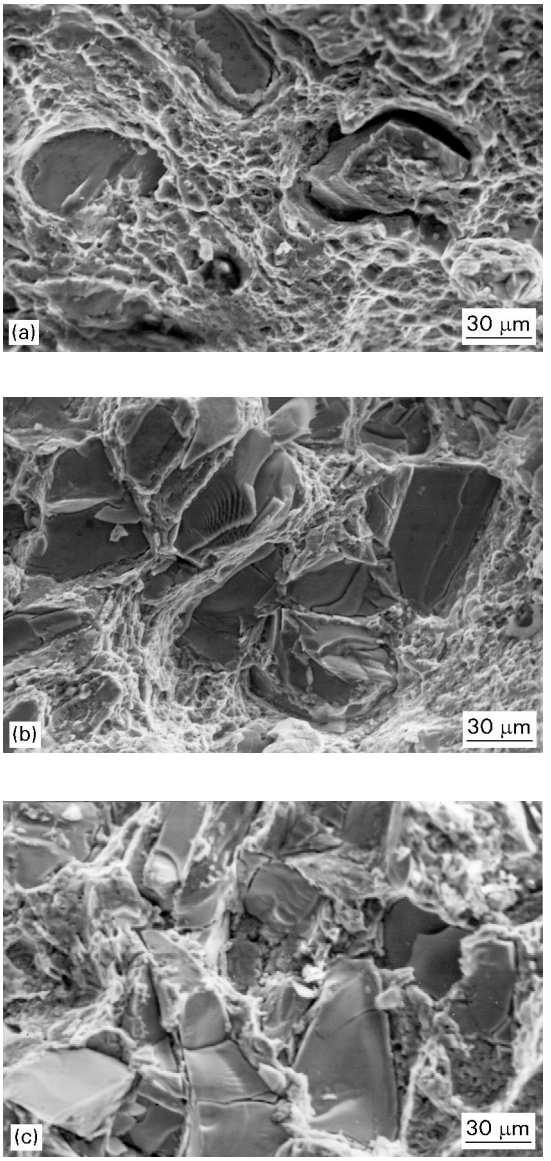

Figure 4 SEM micrograph of 180 mesh SiC_p/6061 Al composite fatigue fracture surface: (a) 10 wt %, (b) 20 wt % and (c) 30 wt %.

4. Conclusions

For the 6061 Al alloy and the SiC_p/6061 Al composites produced by a powder metallurgy method, the following conclusions can be made concerning the results of this study:

(1) The composite was manufactured by CIP at a pressure of 100 MPa, with the air and wax being removed at 400 °C. The sample underwent liquid phase sintering at 620 °C and hot extrusion at 500 °C followed by room temperature rolling. The composite attained the full theoretical

density and had a uniform distribution of the particulates.

(2) The yield strength, tensile strength, and elastic modulus significantly increase with an increase in the fraction of SiC_p particles. However, the elongation decreases.

(3) After several or several tens of fatigue cycles, the specimens reach their highest hardness values and then the specimens exhibit a steady-state behaviour until sudden softening at fracture. This hardening effect was observed in all the composites and also the 6061 Al alloy.

(4) Increasing the content of SiC particles produced more cleavage failure type SiC particles, which resulted in worse fatigue properties.

(5) The large SiC_p particle size enables us to observe particle cracking and cleavage more clearly. Data for the fatigue ductility exponents and fatigue ductility coefficients have been obtained for the SiC_p/6061 Al composites.

Acknowledgement

The authors are grateful for the sponsorship of the National Science Council of the Republic of China under grant NSC-81-0405-E007-15.

References

1. T. M. F. RONALD, *Adv. Mater. Proc.* **144** (1993) 24.
2. T. S. SRIVATSAN, I. A. IBRAHIM, F. A. MOHAMED and E. J. LAVERNIA, *J. Mater. Sci.* **26** (1991) 5965.
3. D. L. McDANELS, *Metall. Trans.* **16A** (1985) 1105.
4. D. MOTT and P. K. LIAW, *ibid.* **19A** (1988) 2233.
5. T. S. SRIVATSAN, *Int. J. Fatigue* **14** (1992) 173.
6. M. LEVIN and B. KARLSSON, *ibid.* **15** (1993) 377.
7. T. S. SRIVATSAN, R. AURADKAR, E. J. LAVERNIA and A. PRAKASH, *Mater. Trans. JIM* **32** (1991) 473.
8. J. LLORCA, S. SURESH and A. NEEDLEMAN, *Metall. Trans.* **23A** (1992) 919.
9. G. M. VYLETEL, D. C. VANAKEN and J. E. ALLISON, *Scripta Metall.* **25** (1991) 2405.
10. J. BONNEN, J. ALLISON and J. JONES, *Metall. Trans.* **22A** (1991) 1007.
11. C. MASUDA and Y. TANAKA, *J. Mater. Sci.* **23** (1992) 413.
12. D. Z. WANG, J. LIU, C. K. YAO, Z. H. HE and L. GENG, *J. Mater. Sci. Lett.* **13** (1994) 957.
13. L. F. COFFIN, *Trans. ASME* **76** (1954) 931.
14. S. S. MANSON, *NASA Technical Note* **12954** 92933.
15. T. S. SRIVATSAN, *Int. J. Fatigue* **13** (1991) 313.
16. T. S. SRIVATSAN, D. LANNING JR and K. K. SONI, *ibid.* **15** (1993) 231.

Received 21 August 1995
and accepted 10 February 1997